Inorg. Chem. **2007**, *46*, 1488–1501

Structure and Bonding of Vanadium(V) Complexes with Hydroxyurea in Aqueous Solution: Density Functional Theory Investigations of Isomers and Intramolecular Rearrangements

Ivana Vinković Vrček,[†] Mladen Biruš,[†] and Michael Bühl*,[‡]

Faculty of Pharmacy and Biochemistry, University of Zagreb, HR-10000, Zagreb, Croatia, and Max-Planck-Institut für Kohlenforschung, Kaiser-Wilhelm-Platz 1, D-45470 Mülheim an der Ruhr, Germany

Received September 8, 2006

Extensive geometry optimizations have been performed at the BP86 level of density functional theory, in order to identify the most stable isomer of pentacoordinated $[VO(OH)UH_2O]^+$ and $[VOU(H_2O)_2]^{2+}$ as well as of hexacoordinated $[VO(OH)U(H_2O)_2]^+$ and $[VOU(H_2O)_3]^{2+}$ complexes (U = hydroxyurea anion). Most of these are conformationally very flexible, with up to 12 isomers within an energy range of 5 kcal/mol. The most stable hexacoordinate forms are characterized by the oxo ligand in trans position to the carbonyl O atom of *U*. Bulk solvent effects on the relative stabilities, estimated from a polarizable continuum model, are indicated to be small and do not affect the energetic sequence of the isomers significantly. Details of the coordination sphere of the most stable isomers in aqueous solution (coordination number, protonation state) have been studied with Car–Parrinello molecular dynamics simulations. The preferred mechanisms of interconversion between selected $[VO(OH)U(H_2O)_2]^+$ isomers, according to the DFT computations, involve proton transfers between H_2O and OH or between O and OH ligands in the coordination sphere of the metal, assisted by a water molecule from the second hydration sphere.

Introduction

Metal ions play an important role in the action mechanism of different drugs.[1] Interest in vanadium coordination chemistry over the past decade has been spurred mainly due to its physiological importance and catalytic abilities.[2] Several biological functions of vanadium have been described, including hormonal, cardiovascular, and antitumor activities.[3] The insulin-enhancing activity of vanadium compounds has received growing interest over the past two decades.[4] The ease of conversion between vanadyl (V(IV)) and vanadate (V(V)), the two forms of vanadium present in equilibrium in the human body, both permits and complicates various interactions with biological molecules. Complexation of aqueous vanadium(V) with organic ligands consequently has been studied intensively.[5] The speciation of the vanadium is of particular interest since it is responsible for the biological activity.[6] Several speciation studies have been carried out on oxovanadium(V) systems,[7−9] dealing with complexation reaction between oxovanadium ions and hydroxamic acids. Hydroxamic acids, RC(=)N(R′)OH, deprotonated to monoanions, bind to the metal ion in a bidentate fashion through the deprotonated hydroxyl and the neutral carbonyl oxygen atoms. The most frequently used hydroxamic acid in human medicine is hydroxyurea (R=NH_2, R′ = H). Hydroxyurea (H*U*) is an S-phase specific inhibitor of ribonucleotide reductase with a broad spectrum of antitumor effects.[10−12] Among other effects, H*U* significantly improves the clinical outcome in patients with sickle cell disease.[13,14]

* Corresponding author fax: + (0)208-306 2996; e-mail: buehl@mpi-muelheim.mpg.de.
[†] University of Zagreb.
[‡] Max-Planck-Institut für Kohlenforschung.

(1) Sigel, H.; Sigel, A. In *Metal Ions in Biological Systems*; Marcel Dekker: New York, 1996; Vol. 31.
(2) Crans, D. C.; Smee, J. J.; Gaidamauskas, E.; Yang, L. *Chem. Rev.* **2004**, *104*, 849−902.
(3) *Vanadium in Biological Systems*; Chasteen, N. D., Ed.; Kluwer: Dordrecht, 1990.
(4) (a) Shechter, Y.; Karlish, S. J. D. *Nature* **1980**, *284*, 556−558. (b) Heyliger, C. E.; Tahiliani, A. G.; McNeill, J. H. *Science* **1985**, *227*, 1474−1477. (c) Reul, B. A.; Amin, S. S.; Buchet, J.-P.; Ongemba, L. N.; Crans, D. C.; Brichard, S. M. *Br. J. Pharm.* **1999**, *126*, 467−477.
(5) Butler, A.; Walker, J. V. *Chem. Rev.* **1993**, *93*, 1937−1944.
(6) Andersson, I.; Angus-Dunne, S.; Howarth, O. W.; Pattersson, L. *J. Inorg. Biochem.* **2000**, *80*, 51−58.
(7) Yamaki, R. T.; Paniago, E. B.; Carvalho, S.; Howarth, O. W.; Kam, W. *J. Chem. Soc., Dalton Trans.* **1997**, 4817−4821.
(8) Bell, J. H.; Pratt, R. F. *Inorg. Chem.* **2002**, *41*, 2747−2753.
(9) Santos, J. M. D. S.; Carvalho, S.; Paniago, E. B.; Duarte, H. A. *J. Inorg. Biochem.* **2003**, *95*, 14−24.

10.1021/ic061699y CCC: $37.00 © 2007 American Chemical Society
Published on Web 01/24/2007

The VO_2^+ cation is the prevailing vanadium(V) species at low pH.[15] Dominant complexes of vanadium(V) with hydroxamic acids at low and neutral pH and at low, physiologicaly relevant, concentrations are of 1:1 stoichiometry with a structure that involves only weak carbonyl coordination.[2] There is still an open question concerning the coordination number about vanadium(V) ion. In contrast to many other metals, the vanadium atom can adopt a variety of different coordination numbers. It generally shows no significant preferences for five-, six-, or seven-coordination; the actual geometry is often highly ligand-dependent. Even well-known vanadium compounds are often poorly described with respect to their stability and structure in aqueous solution.[16]

Concerning the redox properties of the vanadium(V/IV) couple, a main benefit from using oxovanadium(V) as oxidizing agent arises from its pH dependent reduction potential due to the presence of coordinated oxo-ions.[17] Recently, Gabričević et al. have reported a study on the oxidation reaction of hydroxyurea with oxovanadium(V) ions in acidic aqueous solution[18] in order to better understand the behavior of H*U* in solution and, eventually, its therapeutic effectiveness. They have found that the complexation of H*U* by V(V) ions is favored by high acidity owing to the possible protonation of the coordinated oxo ligands, while for the majority of metal ions a high acidity destabilizes the hydroxamato complexes. They reported that in acidic solutions two forms of the mono(hydroxyurea)vanadium(V) complex exist which are the result of two complexation reactions (eqs 1 and 2). These two complexes rapidly equilibrate through the binding/release of one proton characterized by $pK_a = 0.63$ (eq 3).

$$V^{V}O_2^{+} + HU \leftrightarrows V^{V}O(OH)U^{+} \quad (1)$$

$$V^{V}O_2^{+} + HU + H^{+} \leftrightarrows V^{V}OU^{2+} + H_2O \quad (2)$$

$$V^{V}OU^{2+} \leftrightarrows V^{V}O(OH)U^{+} + H^{+} \quad (3)$$

However, kinetic analysis provides no direct information on the binding mode of the ligands, a fact that hampers a more detailed chemical discussion.

In this contribution, we investigate the electronic structure of the complexes formed from the coordination of VO_2^+ by hydroxyurea using density functional theory (DFT), aiming to contribute to the understanding of the metal/ligand interaction mechanism at a molecular level. The main issue in the present study is to describe stable structures of complexes between oxovanadium(V) and hydroxyurea, both monocationic ($VO(OH)U^+$, **1**) and dicationic variants (VOU^{2+}, **2**) according to eq 3, their relative stabilities, and mechanisms of interconversion. As it turns out, both are conformationally very flexible, and care has to be taken in order to identify the most stable structures.

Computational Details

All calculations were performed using the Gaussian03 suite of programs[19] and employed the functional combination according to Becke[20] and Perdew[21] (denoted BP86) together with a fine integration grid (75 radial shells with 302 angular points per shell), the augmented all-electron Wachters' basis[22] on V (8s7p4d, full contraction scheme 62111111/3311111/3111), and 6-31G** on all other elements, denoted as AE1 basis set (except otherwise denoted). This and comparable DFT levels have proven to be quite successful for transition-metal compounds and are well suited for the description of structures, energies, barriers, etc.[23] All structures were fully optimized without symmetry constraints. The nature of the stationary points was verified by computations of the harmonic frequencies at the same level of theory. Transition states were characterized by a single imaginary frequency, and visual inspection of the corresponding vibrational modes ensured that the desired minima are connected. The computed harmonic frequencies were used to evaluate zero-point energies (ZPEs) and thermal corrections to Gibbs free energies as well as enthalpic and entropic contributions. To address bulk solvation effects, the Polarized Continuum model (PCM) of Tomasi and co-workers[24] was applied using the parameters of water. Single point PCM calculations of all complexes were computed at the same level of theory using gas-phase optimized geometries, and in most cases the geometries were subsequently

(10) Zhou, B. S.; Mi, S. X.; Mo, L.; Shih, J.; Tsai, J.; Hu, E.; Hsu, M.; Kay, K.; Yen, Y. *Anticancer Res.* **2002**, *22*, 1369−1377.
(11) Huang, H.; You, J. Y.; Hsu, H. C. *Haematologia* **2002**, *32*, 87−91.
(12) Mason, W. P.; Gentili, F.; Macdonald, D. R.; Hariharan, S.; Cruz, C. R.; Abrey, L. E. *J. Neurosurg.* **2002**, *97*, 341−346.
(13) Charache, S.; Terrin, M. L.; Moore, R. D.; Dover, G. J.; Mcmahon, R. P.; Barton, F. B.; Waclawiw, M.; Eckert, S. V. *Controlled Clin. Trials* **1995**, *16*, 432−446.
(14) Ferguson, R. P.; Arun, A.; Carter, C.; Walker, S. D.; Castro, O. *Am. J. Hematol.* **2002**, *70*, 326−330.
(15) Cruywagen, J. J.; Heyns, J. B. B.; Westra, A. N. *Inorg. Chem.* **1996**, *35*, 1556−1559.
(16) Crans, D. C.; Keramidas, A. D.; Amin, S. S.; Anderson, O. P.; Miller, S. M. *J. Chem. Soc., Dalton Trans.* **1997**, 2799−2812.
(17) (a) Pettersson, L.; Nenner, A.-M.; Anderson, I. *Acta Chem. Scand. A* **1985**, *39*, 453−499. (b) Fabjan, C.; Garche, J.; Harrer, B.; Jörissen, L.; Kolbeck, C.; Philippi, F.; Tomazic, G.; Wagner, F. *Electrochim. Acta* **2001**, *47*, 825−831.
(18) Gabričević, M.; Bešić, E.; Biruš, M.; Zahl, A.; van Eldik, R. *J. Inorg. Biochem.* **2006**, *100*, 1606−1613.
(19) Frisch, M. J.; Trucks, G. W.; Schlegel, H. B.; Scuseria, G. E.; Robb, M. A. Cheeseman, J. R.; Montgomery, J. A., Jr.; Vreven, T.; Kudin, K. N.; Burant, J. C.; Millam, J. M.; Iyengar, S. S.; Tomasi, J.; Barone, V.; Mennucci, B.; Cossi, M.; Scalmani, G.; Rega, N.; Petersson, G. A.; Nakatsuji, H.; Hada, M.; Ehara, M.; Toyota, K.; Fukuda, R.; Hasegawa, J.; Ishida, M.; Nakajima, T.; Honda, Y.; Kitao, O.; Nakai, H.; Klene, M.; Li, X.; Knox, J. E.; Hratchian, H. P.; Cross, J. B.; Bakken, V.; Adamo, C.; Jaramillo, J.; Gomperts, R.; Stratmann, R. E.; Yazyev, O.; Austin, A. J.; Cammi, R.; Pomelli, C.; Ochterski, J. W.; Ayala, P. Y.; Morokuma, K.; Voth, G. A.; Salvafdor, P.; Dannenberg, J. J.; Zakrzewski, V. G.; Dapprich, S.; Daniels, A. D.; Strain, M. C.; Farkas, O.; Malick, D. K.; Rabuck, A. D.; Raghavachari, K.; Foresman, J. B.; Ortiz, J. V.; Cui, Q.; Baboul, A. G.; Clifford, S.; Cioslowski, J.; Stefanov, B. B.; Liu, G.; Liashenko, A.; Piskorz, P.; Komaromi, I.; Martin, R. L.; Fox, D. J.; Keith, T.; Al-Laham, M. A.; Peng, C. Y.; Nanayakkara, A.; Challacombe, M.; Gill, P. M. W.; Johnson, B.; Chen, W.; Wong, M. W.; Gonzalez, C.; Pople, J. A. *Gaussian 03*; Gaussian, Inc.: Wallingford, CT, 2004.
(20) Becke, A. D. *Phys. Rev. A* **1988**, *38*, 3098−3100.
(21) (a) Perdew, J. P. *Phys. Rev. B* **1986**, *33*, 8822−8824. (b) Perdew, J. P. *Phys. Rev. B* **1986**, *34*, 7406−7406.
(22) (a) Wachters, A. J. H. *J. Chem. Phys.* **1970**, *52*, 1033−1036. (b) Hay, P. J. *J. Chem. Phys.* **1977**, *66*, 4377−4384.
(23) See, for instance: Koch, W.; Holthausen, M. C. *A Chemist's Guide to Density Functional Theory*; Wiley-VCH: Weinheim, Germany, 2000; and the extensive bibliography therein.
(24) As implemented in G 03: (a) Barone, V.; Cossi, M.; Tomasi, J. *J. Comput. Chem.* **1998**, *19*, 404−417. (b) Cossi, M.; Scalmani, G.; Rega, N.; Barone, V. *J. Chem. Phys.* **2002**, *117*, 43−54. (c) Cossi, M.; Crescenzi, O. *J. Chem. Phys.* **2003**, *19*, 8863−8872.

optimized in the continuum. Natural bond orbital (NBO) analysis was performed using the NBO 3.1 program[25] as implemented in the GAUSSIAN03 package. Natural charges and bond orders were computed at the same BP86/AE1 level of theory. In order to gauge effects of the exchange-correlation potential on the relative stabilities, single-point energy calculations have been performed on the BP86/AE1 geometries employing AE1 basis and the popular B3LYP hybrid functional.[26] Most of these results, together with optimized coordinates, are collected in the Supporting Information. We have not optimized geometries at the B3LYP level, because this functional has recently been shown to be systematically inferior to BP86 for geometries of transition-metal complexes.[27]

For selected isomers, the geometries were reoptimized at the BP86 level using the Car−Parrinello scheme[28] as implemented in the CPMD program,[29] until the maximum gradient was less than $5 \cdot 10^{-4}$ au (denoted CP-opt). Norm-conserving pseudopotentials were employed that had been generated according to the Troullier and Martins procedure[30] and transformed into the Kleinman-Bylander form.[31] For vanadium, a semicore (or small-core) pseudopotential was used that had performed well in previous applications to vanadate complexes.[32] Periodic boundary conditions were imposed using a cubic supercell with a box size of 13.0 Å. Kohn−Sham orbitals were expanded in plane waves up to a kinetic energy cutoff of 80 Ry.[33] For the complex in vacuo, Car−Parrinello molecular dynamics simulations were performed starting from the equilibrium structure, using a fictitious electronic mass of 600 au and a time step of 0.121 fs. Unconstrained simulations (NVE ensemble) were performed over 2.5 ps at ca. 300 K, the first 0.5 ps of which were taken for equilibration. For the aqueous solutions, the boxes were filled with 62 additional water molecules, yielding a density of 1.0. In order to increase the time step, hydrogen was substituted with deuterium. The systems were equilibrated for 0.5 ps maintaing a temperature of 300(±50) K via velocity rescaling and were then propagated without constraints for up to 6 ps.

Results and Discussion

This part is organized as follows: first, we present a detailed conformational analysis of the title complexes in the gas phase and in a bulk continuum model, followed by an assessment of their relative thermodynamic stabilities as emerging from these static computations. Next, we discuss thermal and explicit solvation effects on two prototypical complexes by means of Car−Parrinello molecular dynamics (CPMD) simulations in aqueous solution. Subsequently, we investigate selected pathways for interconversion of low-energy isomers, and finally, we provide a brief discussion of the electronic structure of selected complexes in terms of suitable population analyses.

(25) Glendening, E. D.; Reed, A. E.; Carpenter, J. E.; Weinhold, F. NBO (version 3.1).
(26) (a) Becke, A. D. *J. Chem. Phys.* **1993**, *98*, 5648−5642. (b) Lee, C.; Yang, W.; Parr, R. G. *Phys. Rev. B* **1988**, *37*, 785−789.
(27) Bühl, M.; Kabrede, H. *J. Chem. Theory Comput.* **2006**, *2*, 1282−1290.
(28) Car, R.; Parrinello, M. *Phys. Rev. Lett.* **1985**, *55*, 2471−2474.
(29) *CPMD Version 3.7.0*; Copyright IBM Corp. 1990−2001, Copyright MPI für Festkörperforschung Stuttgart 1997−2001.
(30) Troullier, N.; Martins, J. L. *Phys. Rev. B* **1991**, *43*, 1993−2006.
(31) Kleinman, L.; Bylander, D. M. *Phys. Rev. Lett.* **1982**, *48*, 1425−1428.
(32) (a) Bühl, M.; Schurhammer, R.; Imhof, P. *J. Am. Chem. Soc.* **2004**, *126*, 3310−3320. (b) Bühl, M. *Inorg. Chem.* **2005**, *44*, 6277−6283.
(33) The notations AE1 and CP-opt thus denote two different approximations for constructing the Kohn-Sham wavefunction, namely one based on an all-electron basis set moving with the atoms and the other on atomic pseudopotential cores swimming in a sea of periodic plane-waves.

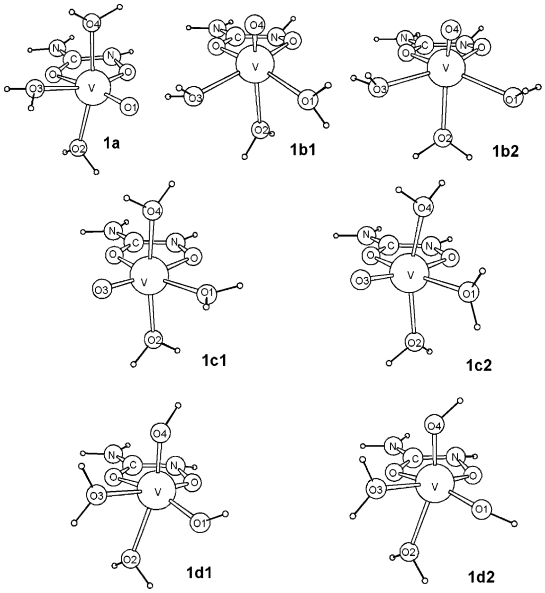

Figure 1. Optimized geometries for dicationic complexes of V(V) with H*U* calculated at the BP86/AE1 level of theory.

Structures and Energetics. The following discussion is based on the structures and energies reported in Figures 1−5, in Tables 1−5, and in the Supporting Information. The latter contains the coordinates of all geometries optimized in the gas phase as well as selected geometrical parameters and additional energetic data.

(a) $[VOU(H_2O)_3]^{2+}$. Experimental results published from our laboratory show that in aqueous solution, hydroxyurea anion chelates the vanadium(V) forming a 5-membered ring system. The above general formula ($[VOU(H_2O)_3]^{2+}$ - **1**) covers numerous possible structures of the formed complex-(es), consisting of one oxo ligand and three water molecules or two hydroxo ligands and two water molecules. These two types of complexes cannot be discerned experimentally from spectroscopic and potentiometric experimental data alone, and elucidation of the stereochemistry of these ligands about the metal center is even more difficult. For instance, the oxo, or hydroxo, ligands may be in axial or equatorial position-(s) with respect to the ring moiety of the chelating hydroxyurea unit,[34] while H_2O molecules complete the six-coordination.

In order to address these questions computationally, unconstrained geometry optimizations were carried out from 96 starting geometries generated from all conceivable mutual orientations of the different ligand atoms about the metal center and from a number of rotamers arising from rotations of the water ligands about the V−O bonds. The optimizations converged to five distinct minima shown in Figure 1. Tables 1 and S1 (in the Supporting Information) summarize the relative energies (both in the gas-phase and from PCM calculations) and key geometric parameters, respectively. We have found one structure with an equatorial oxo ligand *trans* to the carbonyl oxygen (**1a**), two structures with the oxo group in axial position relative to the ring moiety and

(34) Equatorial and axial denote positions with respect to the idealized plane formed by the V−O−C−N−O chelate ring.

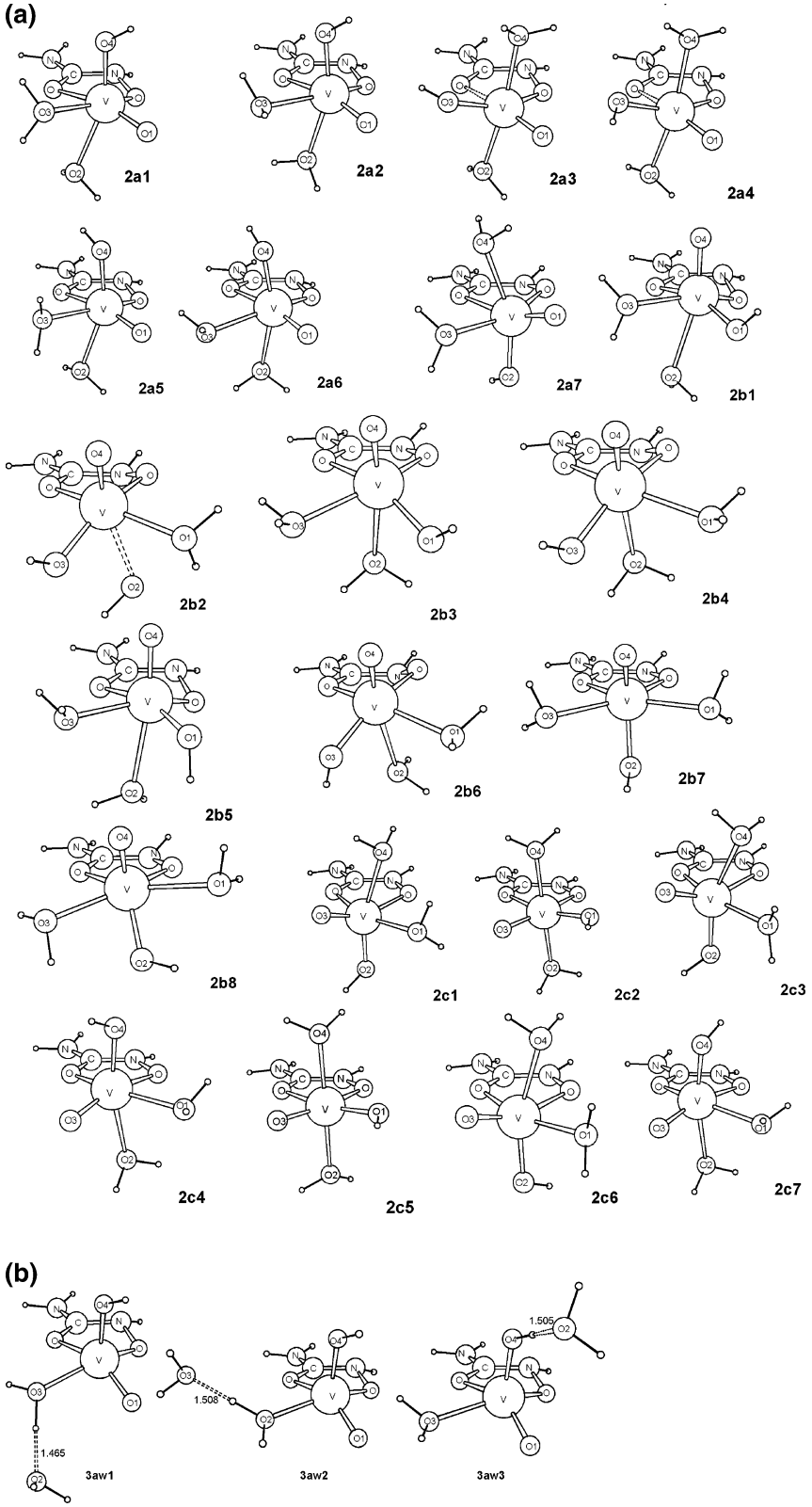

Figure 2. a. Optimized geometries for the hexacoordinated monocationic complexes of V(V) with H*U* calculated at the BP86/AE1 level of theory. b. Optimized geometries (BP86/AE1 level) for microsolvated pentacoordinated monocationic complexes of V(V) with H*U*, arising from water detachment from the hexacoordinated metal in species **2**; isomer **3aw2** was obtained during attempted optimization of an isomeric species similar to **2b4**, **3aw1**, and **3aw3** after optimizing two snapshots from CPMD simulations of **2a1** (see text).

different water orientations (**1b1** and **1b2**), and two structures with the oxo atom *cis* to the carbonyl oxygen (**1c1** and **1c2**).

The most stable of these, **1a**, has an equatorial oxo group relative to the ring moiety and *trans* to the carbonyl oxygen with a slightly distorted ring plane (dihedral angle O−N−C═O is 4.05°). The other isomers with an equatorial oxo ligand *cis* to the carbonyl oxygen were higher in energy than **1a** by 11.3−12.3 kcal/ mol, whereas complexes with axial

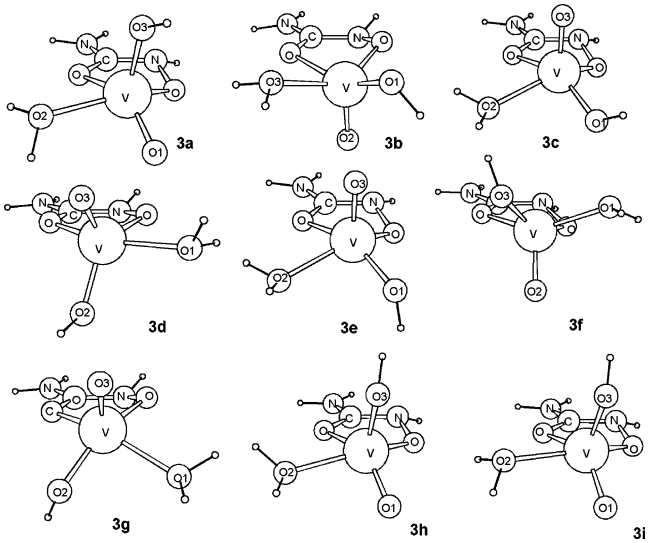

Figure 3. Optimized geometries for pentacoordinate monocationic complexes of V(V) with H*U* calculated at the BP86/AE1 level of theory.

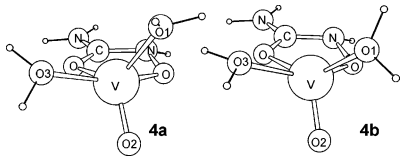

Figure 4. Optimized two geometries for pentacoordinate dicationic complexes of V(V) with H*U* calculated at the BP86/AE1 level of theory.

Table 1. Relative Energies (in kcal/mol) from Gas-Phase BP86/AE1 and PCM/ BP86/AE1//BP86/AE1 Calculations

species	ΔE,[a] kcal/mol	ΔE,[b] kcal/mol	ΔE,[c] kcal/mol	ΔE,[d] kcal/mol
1a	0	0	0	0
1b1	5.1	5.8	5.1	5.3
1b2	7.3	8.9	8.3	7.5
1c1	11.3	13.8	13.0	13.7
1c2	12.3	15.1		13.8
1d1	9.1	11.7		15.7
1d2	9.6	12.5		16.8

[a] Relative energies calculated at the BP86/AE1 level relative to the most stable structure. [b] Relative energies calculated at the single point PCM/BP86/AE1//BP86/AE1 level relative to the most stable structure. [c] Relative energies calculated at the PCM/BP86/AE1 level relative to the most stable structure (only the most stable structures have been optimized in the continuum). [d] Relative energies calculated at the single point B3LYP/AE1//BP86/AE1 level relative to the most stable structure

oxo ligand are 5.1−7.3 kcal/mol higher in energy than **1a**. Interestingly, almost half of the starting structures with equatorial oxo ligands relative to the ring and *cis* to the carbonyl oxygen converged to the isomer **1b2** by rotation of oxo and water ligands around the vanadium center during optimization. In general, the distances between vanadium and the oxo group (around 1.58 Å) or the water ligands (2.06−2.19 Å) are in good accord with other results reported for complexes of oxovanadium and hydroxamic acids.[8,9,35] In **1a**, **1b1**, and **1b2**, wherein the oxo ligand is in the *cis* position to O(N), the V−O(N) bond distances are shorter than the V−O(═) distances by approximately 0.15 Å, while they are longer by 0.04−0.06 Å in **1c1** and **1c2**, where the oxo ligand is in the *trans* position to O(N).

(35) Duarte, H. A.; Paniago, E. B.; Carvalho, S.; De Almeida, W. B. *J. Inorg. Biochem.* **1998**, *72*, 71−77.

Table 2. Relative Energies (in kcal/mol) from Gas-Phase BP86/AE1 (ZPE Correction Included) and PCM/BP86/AE1//BP86/AE1 Calculations

species	ΔE,[a] kcal/mol	ΔE,[b] kcal/mol	ΔE,[c] kcal/mol	species	ΔE,[a] kcal/mol	ΔE,[b] kcal/mol	ΔE,[c] kcal/mol
2a1	0	0	0	**2b7**	8.5	11.0	10.4
2a2	0.7	1.9	0.9	**2b8**	9.1	12.5	11.0
2a3	1.8	1.0	0.5	**2c1**	8.0	11.6	
2a4	2.2	2.8	1.7	**2c2**	8.4	12.4	
2a5	2.8	0.9	0.6	**2c3**	8.7	13.1	
2a6	3.6	2.6	1.9	**2c4**	9.4	14.2	
2a7	4.2	1.9	1.1	**2c5**	9.5	11.3	
2b1	0.8	2.7	1.8	**2c6**	10.4	12.1	
2b2	3.3	4.9		**2c7**	11.5	13.6	
2b3	4.2	5.6	4.7	**3aw1**	−4.7	−1.9	
2b4	4.8	7.0	5.5	**3aw2**	−2.0	0.7	
2b5	5.1	5.0	4.1	**3aw3**	−1.1	1.9	
2b6	8.1	6.5	6.0				

[a] Relative energies calculated at the BP86/AE1 level relative to the most stable structure. [b] Relative energies calculated at the single point PCM/BP86/AE1//BP86/AE1 level relative to the most stable structure. [c] Relative energies calculated at the PCM/BP86/AE1 level relative to the most stable structure (only the most stable structures have been optimized in the continuum; optimization for **2b2** failed to converge).

Table 3. Relative Energies (in kcal/mol) from Gas-Phase BP86/AE1 and PCM/ BP86/AE1//BP86/AE1 Calculations

species	ΔE,[a] kcal/mol	ΔE,[b] kcal/mol	ΔE,[c] kcal/mol	ΔE,[d] kcal/mol
3a	0	0	0	0
3b	0	0.02	0.02	0.8
3c	1.4	1.4	1.3	0.8
3d	1.7	2.7	-	1.1
3e	3.7	2.2	2.0	3.0
3f	3.7	2.5	2.0	4.0
3g	4.1	2.5	2.6	4.1
3h	4.2	1.5	2.0	4.6
3i	4.2	1.6	2.0	4.7

[a] Relative energies calculated at the BP86/AE1 level relative to the most stable structure. [b] Relative energies calculated at the single point PCM/BP86/AE1//BP86/AE1 level relative to the most stable structure. [c] Relative energies calculated at the PCM/BP86/AE1 level relative to the most stable structure (optimization for **3d** failed to converge). [d] Relative energies calculated at the single point B3LYP/AE1//BP86/AE1 level relative to the most stable structure.

Duarte et al.[35] have reported that in the case of the neutral complex between oxovanadium(V) and acetohydroxamic acid (*AH*), $VO_2A(H_2O)_2$, an intramolecular proton transfer can occur from the H_2O ligand to one of the oxo ligands, and this new species ($VOA(OH)_2(H_2O)$) is about 12 kcal/mol more stable than the structure in which two oxo ligands and the H_2O molecule are coordinated to the vanadium center. We have investigated possible structures of our dicationic hydroxyurea complex **1**, having two hydroxy and two H_2O ligands resulting from an analogous proton transfer. The two most stable isomers of these are **1d1** and **1d2** (Figure 1), which are, contrary to the findings of Duarte et al., 10.6 kcal/mol and 11.5 kcal/mol, respectively, less stable than the most stable oxo complex, structure **1a**.

(b) $[VO(OH)U(H_2O)_2]^+$. In the unprotonated monocationic complex from eq 1 (**2**), both the single oxo and OH groups may be in axial or equatorial position with respect to the chelate ring formed by the hydroxamate, with two H_2O molecules filling up the remaining two binding sites to

Table 4. Relative Energies (ΔE in kcal/mol) from Gas-Phase BP86/AE1 and PCM/ BP86/AE1//BP86/AE1 Calculations for Pentacoordinated Monocationic V(V) Complexes with H*U*

level	**4a**	**4b**
BP86/AE1	0	0.8
PCM/BP86/AE1//BP86/AE1	0	0.8
B3LYP/AE1//BP86/AE1	0	1.2

Table 5. a. Dehydration Free Energies, $\Delta G^0_{aq,dehydration}$, and b. Deprotonation Free Energies, $\Delta G^0_{aq,deprot}$, of Complexes Studied at the BP86/AE1 Level of Theory (in kcal/mol)

a.

reaction	ΔG^0_{aq} [a]	ΔG^0_{aq} [b]
1a → **4a** + H_2O	17.9	15.3
1b → **4a** + H_2O	13.2	10.6
2a1 → **3a** + H_2O	6.2	4.9
2b2 → **3g** + H_2O	4.7	4.5
2a2w → **2a2** + H_2O		1.7
2a4w → **2a4** + H_2O		6.7
2a1 → **3aw1**		-2.9

b.

reaction	ΔG^0_{aq} [a]	ΔG^0_{aq} [b]
1a ⇆ **2a1** + H^+	−26.1	−28.6
1a + H_2O ⇆ **2a1** + H_3O^+	3.8	−0.6
4a ⇆ **3a** + H^+	−37.9	−45.6
4a + H_2O ⇆ **3a** + H_3O^+	−7.9	−1.0

[a] Calculated from PCM using cavity built from the United Atom (UA0) model. [b] Calculated from PCM employing an all-atom cavity using the radii from the UFF force field.

form a hexacoordinated complex. Because in **2** there are, for a given vanadium−hydroxamate moiety, three types of monodentate O-donors to be distributed over 4 binding sites, the number of possible isomers is much larger than for **1**. Allowing for possible rotamers of H_2O and OH ligands, we screened more than 300 starting structures. From these, we could locate 23 different minima (not counting enantiomers). Their structures and relative energies are collected in Figure 2a and Tables 2 and S2a−c.

Among all these minima, 5 structures have an equatorial oxo atom *trans* to the carbonyl oxygen and the hydroxyl group *axial* relative to the ring moiety (**2a1, 2a2, 2a5, 2a6**, and **2a7**); 2 structures have equatorial oxo and OH groups *trans* and *cis*, respectively, to the carbonyl oxygen (**2a3** and **2a4**); 6 structures have an axial oxo group relative to the ring moiety and an equatorial hydroxyl group either *cis* or *trans* to the carbonyl oxygen (**2b1**, **2b2**, **2b3**, **2b4**, **2b5**, and **2b6**); 2 structures have axial oxo and hydroxyl groups (**2b7** and **2b8**); 5 structures have the equatorial oxo group *cis* to the carbonyl oxygen and an axial hydroxyl group (**2c1**, **2c3**, **2c4**, **2c6**, and **2c7**); and 2 structures have equatorial oxo and OH groups *cis* and *trans*, respectively, to the carbonyl oxygen (**2c2** and **2c5**). All these structures span the energy range of ca. 12−13 kcal/mol, both in the gas phase and in the polarizable continuum. In general, structures with equatorial oxo ligands *trans* to the carbonyl oxygen are energetically the most favorable both for **1** and **2** (see for comparison Tables 1 and 2). The structures with equatorial oxo ligand *cis* to the carbonyl oxygen were calculated as the least stable isomers. Both hexacoordinated forms, protonated **1** and deprotonated **2**, have distorted tetragonal bipyramidal geometries. The calculated V−OH_2 distances are similar in all cases. In **2**, the V−OH distances are about 0.2 Å shorter than the V−OH_2 separations and about 0.2 Å longer than the V═O bond lengths. The V−OH_2 distances indicate reasonably strongly bonded water molecules occupying the fifth and sixth coordination position around the vanadium center. Again, in all complexes of the **2a** and **2b** series (structures from **2a1**−**2b8**), wherein the oxo ligand is in the *cis* position to O(N), the V−O(N) bonds are shorter than the V−O(C) distances, while in the complexes of the **2c** series (from **2c1**−**2c7**), where the oxo ligand is in the *trans* postion to O(N), the opposite is found.

(c) Pentacoordinated Isomers ([VO(OH)*U*(H_2O)]$^+$ and [VO*U*(H_2O)$_2$]$^{2+}$). In the case of **2**, several starting structures with an equatorial oxo or hydroxo ligands *cis* to the carbonyl oxygen converged to pentacoordinated species where one water ligand was expelled from the coordination sphere of the metal, forming a hydrogen bond to the remaining water ligand (for example **3aw2** in Figure 2b). The most stable of this kind of structures (**3aw2**) is only 2 kcal mol^{-1} less stable than the most stable **2a1**. In addition, following the CPMD simulations for **2a1** (see below), two additional microsolvated 5-coordinate complexes were located that were even slightly more stable than **2a1** in the gas phase, **3aw1** and **3aw3** (shown in Figure 2b). In these cases, apparently, the binding energy of this ligand at the metal center is lower than the strength of the hydrogen bond formed. In order to estimate the bond strength of one water ligand in **1** and **2**, we have computed the pristine pentacoordinated complexes [VO(OH)-*U*(H_2O)]$^+$ (**3**) and dicationic [VO*U*(H_2O)$_2$]$^{2+}$ (**4**) as well. In order to find the most stable minimum in both cases, again a large number of possible structures were initially considered, taking the possibility into account that five-coordinate complexes may adopt idealized trigonal bipyramidal (tbp) or square pyramidal (sp) geometries.

For **3**, 64 starting structures were considered, which optimized to nine different minima, the structures and relative energies of which are given in Figure 3 and Tables 3 and S3. The most stable structure is a distorted trigonal bipyramid with the oxo, OH, and carbonyl oxygen atoms spanning the trigonal base and with the water ligand and the O(N) group in pseudoaxial positions (**3a** in Figure 3).

After protonation of these monocationic pentacoordinated complexes, 32 possible geometries were optimized which led to only two minima (**4a** and **4b**) presented in Figure 4. Relative energies as well as selected geometrical parameters are given in Table 4.

Classification of the coordination mode in the pentacoordinated species as tbp or sp is not always straightforward, since there can be an essentially continuous spectrum in between both idealized arrangements.[36] Most isomers of **3** and **4** can be classified as distorted tbp structures, but some have also a noticeable sp character with the oxo ligand in apical position. That both variants can be of comparable

(36) See, for instance: (a) Zabrodsky, H.; Peleg, S.; Avnir, D. *J. Am. Chem. Soc.* **1992**, *114*, 7843−7851. (b) Addison, A. W.; Rao, T. N.; Reedijk, J.; van Rijn, J.; Verschoor, G. C. *J. Chem. Soc., Dalton Trans.* **1984**, 1349−1356. (c) Alvarez, S.; Llunell, M. *J. Chem. Soc., Dalton Trans.* **2000**, 3288−3303.

stability is best exemplified in the case of **3a** (predominantly tbp) and **3b** (large sp character), which are essentially isoenergetic. The higher conformational flexibility of penta- vs hexa-coordinated complexes is also reflected in the much smaller spread of relative energies in the former (ca. 4 kcal/mol for **3a**−**3f,** less than 1 kcal/mol for **4a**/**4b**) than in the latter (ca. 12−14 kcal/mol). Upon protonation of **3**, e.g. on going from **3a** to **4a**, the calculated V═O and V−OH_2 bond distances decrease by about 0.02 and 0.05 Å, respectively.

So far, discussion of relative energies of the various isomers has been based solely on results obtained with the BP86 functional (which usually performs very well for this purpose[23]). In order to assess the sensitivity of the relative stabilities on the particular exchange-correlation functional, we have performed single-point energy calculations with the popular B3LYP combination. As can be seen from the data included in Tables 1, S2a, 3, and 4, very similar results are obtained with both functionals, both qualitatively and quantitatively: individual changes in relative energies rarely exceed 1 kcal/mol on going from one level to the other, and the lowest isomers remain the same in each case. Therefore we note that there is no pronounced dependency of the results toward the particular flavor of DFT, and we will continue to discuss the BP86 data in the following.

To conclude this section, oxovanadium(V) complexes with hydroxyurea can be conformationally very flexible, in particular in the case of five-coordination.[37] In addition to the general distribution of the ligands over the available coordination sites, the stability of the complexes can also depend strongly on the specific orientations of the water and hydroxy ligands. For instance, structures with the same ligand distribution but different orientation of water ligands can differ by up to 3.4 kcal/mol in energy (compare, for example, **2b1** and **2b3**). Thus, a full conformational analysis is necessary in order to identify the most stable isomer for a given complex. Bulk solvent effects estimated from a PCM are indicated to be of minor importance for the relative energies. While it is well possible that specific interactions with the protic solvent water could modify the energetic sequence of the isomers, we are confident that the lowest minima located in this study, **1a**, **2a1**, **3a**, and **4a**, will be among the principal components in the equilibria describing the speciation of this system. The common structural motif in these structures is an equatorial oxo atom *trans* to the carbonyl oxygen of the hydroxamate chelate ring or, for tbp-type five-coordinated complexes, the presence of both donor atoms in the (idealized) trigonal plane.

Thermodynamics. The evaluation of the solvent effects has been carried out by energy calculations over the BP86/AE1 geometries using polarizable continuum model (PCM)[38] at the same level of theory. The properties obtained for the molecules in the solvent phase are referred to as "aqueous phase". We have examined the stability of the six-coordinated complexes with respect to the loss of one water molecule as well as deprotonation reactions of complexes **1a** and **4a**.

The standard free energies of dehydration of six-coordinate species **1a** and **2a1** (affording **4a** and **3a**, respectively, and a separated water molecule) in water ($\Delta G^0_{\mathrm{aq,dehydration}}$) are defined as

$$\Delta G^0_{\mathrm{aq,dehydration}} = \Delta G^0(\mathbf{4a}_{\mathrm{aq}}) + \Delta G^0(\mathrm{H_2O_{aq}}) - \Delta G^0(\mathbf{1a}_{\mathrm{aq}}) \quad (4a)$$

$$\Delta G^0_{\mathrm{aq,dehydration}} = \Delta G^0(\mathbf{3a}_{\mathrm{aq}}) + \Delta G^0(\mathrm{H_2O_{aq}}) - \Delta G^0(\mathbf{2a1}_{\mathrm{aq}}) \quad (4b)$$

In general, the most stable hexacoordinated chelates (structures **1a** and **1b1** in Figure 1 and **2a1** and **2a2** in Figure 2a) appear to be stable toward the loss of one water molecule affording pentacoordinated V(V) chelates (structures **3a** and **3g** in Figure 3 and **4a** in Figure 4), cf. the positive free energies of dehydration ($\Delta G^0_{\mathrm{aq,dehydration}}$) in Table 5a. The computed dehydration energies for dicationic complexes are much larger than for the corresponding monocationic complexes, consistent with a larger electrostatic stabilization of such dicationic complexes. Thus, the computed dissociation energies for the processes **2a1** → **3a** + H_2O and **2b2** → **3g** + H_2O are very low (4.9 kcal/mol and 4.5 kcal/mol at the BP86/AE1 level, respectively). These values are comparable to that of typical systems involving hydrogen-bonded water molecules.

However, when comparing relative free energies (including solvation) of six- and microsolvated five-coordinate monocations, the latter can be more stable, see the last entry in Table 5a. Apparently, the equilibrium between five-coordinated **2** and six-coordinated **3** in solution is too finely balanced for the simple continuum model.[39] Quite likely, larger cluster models with a complete additional hydration sphere would have to be included within the polarizable continuum for more conclusive results. Anticipating a plethora of possible minima for such fully hydrated clusters, we did not pursue this route further and resorted to MD simulations, the results of which will be discussed in the next section.

From the results in Table 5a it is also apparent that the PCM results can be quite sensitive to details of the construction of the molecular cavity (compare, where available, the two values in each row), a common problem with this kind of computation. For the dicationic complexes with their larger water binding energies, these uncertainties are probably not large enough to change the qualitative result, namely that six-coordination should prevail in water.

(37) (a) Kitchen, D. B.; Allen, L. C. *J. Phys. Chem.* **1989**, *93*, 7265−7269. (b) Krauss, M.; Stevens, W. J. *J. Am. Chem. Soc.* **1990**, *112*, 1460−1466. (c) Garmer, D. R.; Krauss, M. *J. Am. Chem. Soc.* **1992**, *114*, 6487−6493. (d) Probst, M. M. *J. Mol. Struct. (THEOCHEM)* **1992**, *253*, 275−285.

(38) (a) Barone, V.; Cossi, M.; Tomasi, J. *J. Comput. Chem.* **1998**, *19*, 404−417.(b) Cossi, M.; Scalmani, G.; Rega, N.; Barone, V. *J. Chem. Phys.* **2002**, *117*, 43−54. (c) Cossi, M.; Crescenzi, O. *J. Chem. Phys.* **2003**, *119*, 8863−8872.

(39) For instance, the reaction **3aw** → **3a** + H_2O should be thermoneutral in water, as it just describes the exchange of one solvent molecule from the second hydration sphere with one from the bulk. In contrast, the PCM data in Table 5 would a predict a driving force of as much as +8.8 kcal/mol for this process.

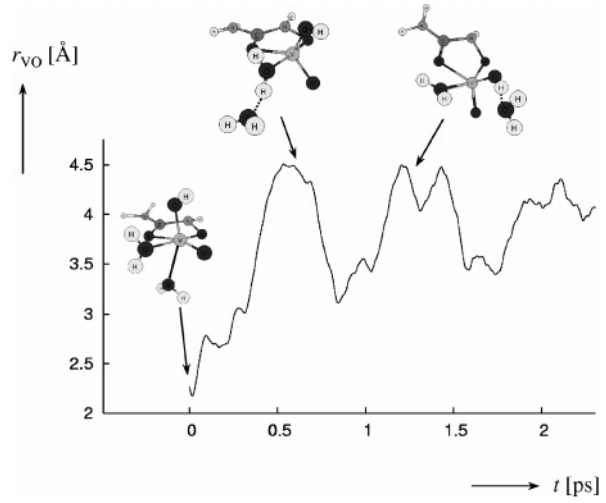

Figure 5. Time-evolution of the V−O2 distance in a CPMD simulation of gaseous **2a1** (*trans* to OH in the starting structure depicted on the left-hand side), together with selected snapshots from the trajectory.

Scheme 1

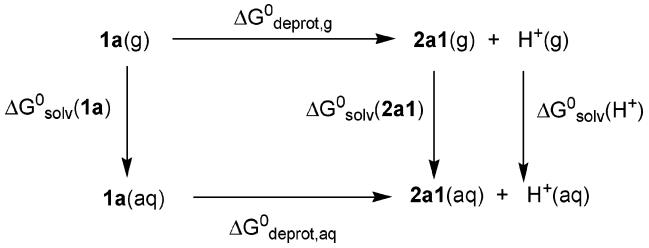

Turning now to the equilibria between dicationic species **1a** or **4a** and monocationic **2a1** or **3a**, respectively, the corresponding standard free energy of deprotonation in water ($\Delta G^0_{aq,deprot}$) can be evaluated via the usual thermodynamic cycles,[40,41] one example of which is depicted in Scheme 1, which results in

$$\Delta G^0_{aq,deprot} = \Delta G^0(\mathbf{2a1}_{aq}) + \Delta G^0(H^+_{aq}) - \Delta G^0(\mathbf{1a}_{aq}) \quad (5a)$$

$$\Delta G^0_{aq,deprot} = \Delta G^0(\mathbf{3a}_{aq}) + \Delta G^0(H^+_{aq}) - \Delta G^0(\mathbf{4a}_{aq}) \quad (5b)$$

where $\Delta G^0(\mathbf{X}_{aq})$ and $\Delta G^0(H^+_{aq})$ are the standard free energy of each species[42] in water. The latter can be written by the sum of the gas-phase standard free energy ΔG^0_g and the standard free energy of solvation in water ΔG^0_{solv} (Scheme 1):

$$\Delta G^0_{aq} = \Delta G^0_g + \Delta G^0_{solv} \quad (6)$$

In this approach, $\Delta G^0(H^+_{aq})$ is taken from experiment.[40] Alternatively, we have evaluated the deprotonation via equations of the type **1a** + H_2O ⇆ **2a1** + H_3O^+, affording

$$\Delta G^0_{aq,deprot} = \Delta G^0(\mathbf{2a1}_{aq}) + \Delta G^0(H_3O^+_{aq}) - \Delta G^0(\mathbf{1a}_{aq}) - \Delta G^0(H_2O_{aq}) \quad (7a)$$

$$\Delta G^0_{aq,deprot} = \Delta G^0(\mathbf{3a}_{aq}) + \Delta G^0(H_3O^+_{aq}) - \Delta G^0(\mathbf{4a}_{aq}) - \Delta G^0(H_2O_{aq}) \quad (7b)$$

where all ΔG values are computed on an equal footing. A similar approach has recently been advocated by Klamt and co-workers.[43] The deprotonation energies for complexes **1a** and **4a**, obtained with both variants, are given in Table 5b.

The computed deprotonation energies can be converted to pK_a values,[40] which for processes **1a** ⇆ **2a1** + H^+ and **1a** + H_2O ⇆ **2a1** + H_3O^+ amount to −20.9 and −0.43, respectively. In comparison to the experimental value of 0.63,[18] both computed pK_a values have the wrong sign, but the latter one is close enough to the experimental one, probably due to the cancellation of errors in the thermodynamic cycle given by equation **1a** + H_2O ⇆ **2a1** + H_3O^+. It is well-known that for highly charged transition-metal complexes, the calculation of hydration energies and, in particular, of the pK_a values resulting from ligand deprotonation poses a considerable challenge to combined density functional and continuum dielectric models.[44] Adopting a reasonable discrete supramolecular cluster model (which includes the second solvation shell) inside the cavity of the dielectric continuum has been suggested as a possible way to improve the accuracy of such static computations.[44] For qualitative purposes, we have adopted an MD-based approach, in which the solvent is described as a dynamic ensemble, the results of which will be discussed in the following.

Molecular Dynamics Simulations. We performed CPMD simulations for two prototypical representatives, **1a** and **2a1**. The former dication remained stable in the gas phase for a total of 2.1 ps. No rearrangements of the heavy-atom skeleton occurred during that time, whereas the orientation of the three water molecules was quite flexible. One of these (O3 in Figure 1) fulfilled a complete rotation about the V−O bond during this short simulation time.

Monocationic **2a1**, on the other hand, turned out to be unstable in the gas phase. As illustrated in Figure 5, the water

(40) (a) Topol, I. A.; Tawa, G. J.; Burt, S. K.; Rashin, A. A. *J. Phys. Chem. A* **1997**, *101*, 10075−10081. (b) Topol, I. A.; Tawa, G. J.; Caldewell, K. A.; Esseinstat, M. A.; Burt, S. K. *J. Phys. Chem. A* **2000**, *104*, 9619−9624. (c) Liptak, M. D.; Shields, G. C. *J. Am. Chem. Soc.* **2001**, *123*, 7314−7319.

(41) (a) Kallies, B.; Mitzner, R. *J. Phys. Chem. B* **1997**, *101*, 2959−2967. (b) Lim, C.; Bashford, D.; Karplus, M. *J. Phys. Chem.* **1991**, *95*, 5610−5620.

(42) The standard Gibbs free energy of each species in the gas phase in its standard state (ideal gas at 1 atm and 298 K) is obtained by the following equation: $\Delta G^0_g = E_{0K}$ + ZPE + $\Delta\Delta G_{0\rightarrow 298K}$. The total energy of the molecule at 0 K (E_{0K}) is calculated at the optimum geometry from BP86. The zero-point energy (ZPE) and the Gibbs free energy change from 0 to 298 K at 1 atm ($\Delta\Delta G_{0\rightarrow 298K}$) are calculated from the vibrational frequencies using BP86. Translational and rotational free energy contribution is also calculated in the ideal gas approximation. The standard free energy of solvation in water [e.g. $\Delta G^0(\mathbf{2}_{aq})$ and $\Delta G^0(\mathbf{1}_{aq})$] was calculated as a difference between the SCF energies from gas phase and solvated calculations. To obtain $\Delta G^0_{aq,deprotonation}$ requires the standard free energy of a proton in water, $\Delta G^0(H^+_{aq})$. The values for $\Delta G^0_g(H^+)$ and $\Delta G^0_{solv}(H^+)$ are derived from experiment. We have used the values $\Delta G^0_g(H^+) = -6.28$ kcal/mol and $\Delta G^0_{solv}(H^+) = -264.61$ kcal/mol.[40] The values of calculated ΔG^0_g must be converted from reference state of 1 atm to a reference state of 1 M which is accomplished using the equation: ΔG^0_g (1 M) = ΔG^0_g (1 atm) + RT ln(24.46).

(43) (a) Klamt, A.; Eckert, F.; Diedenhofen, M.; Beck, M. E. *J. Phys. Chem. A* **2003**, *109*, 9380−9386. (b) Klamt, A.; Eckert, F. *J. Comput. Chem.* **2006**, *27*, 11−19.

(44) Li, J.; Fisher, C. L.; Chen, J. L.; Bashford, D.; Noodleman, L. *Inorg. Chem.* **1996**, *35*, 4694.

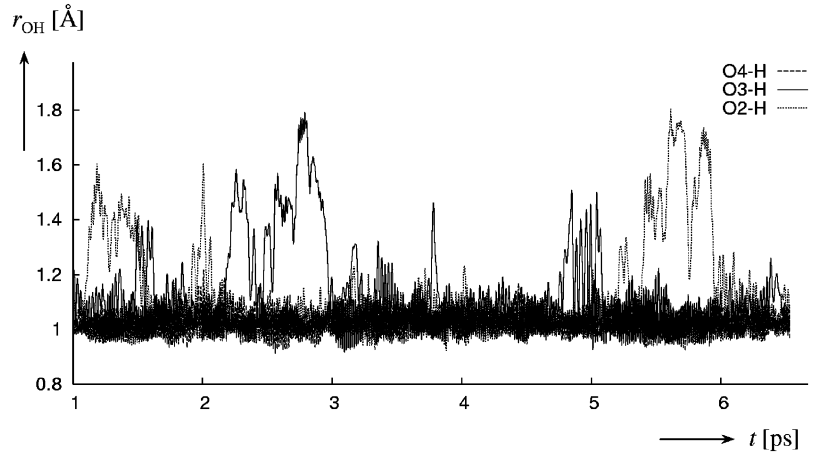

Figure 6. Time-evolution of the six OH distances in a CPMD simulation of **1a** immersed in water with an additional proton. Two water ligands reversibly transfer protons to the solvent.

molecule trans to the OH group rapidly detached from the metal (within a few hundred fs), affording five-coordinated variants of **3a** and **3b** with that water molecule hydrogen-bonded to another water and the OH ligand, respectively. Starting from the two snapshots depicted at the top of Figure 5, the corresponding minima (**3aw1** and **3aw3**, respectively) were located at the BP86/AE1 level. At that level, these minima indeed turned out to be slightly more stable than six-coordinate **2a1**, namely by 4.75 and 1.09 kcal/mol (including zero-point energy correction). This situation is completely analogous to that encountered in $VO_2(H_2O)_4^+$ and VO(OH)(glygly)(H_2O), where the corresponding microsolvated $VO_2(H_2O)_3^+$ and VO(OH)(glygly) five-coordinated species turned out to be more stable in the gas phase.[45,32b] Apparently, the binding energy of an additional water ligand to monocationic (or neutral) five-coordinate vanadate complexes is too small to compete with the rather strong hydrogen bond between these species, at least at the DFT level employed.[46]

When six-coordinate **2a1** was immersed in a periodic water box, the water ligand *trans* to the OH group (O2 in Figure 2a) also appeared to be somewhat more labile than that *trans* to the hydroxamato oxygen (O3). The bonding to both water ligands appears to be reinforced upon solvation, cf. the mean V−O2 and V−O3 distances of 2.20(14) Å and 2.00(8) Å, respectively, averaged over a total of 5 ps of simulation after 0.5 ps of equilibration (standard deviations in parentheses). These distances are significantly shorter than the CP-opt equilibrium values of 2.279 Å and 2.113 Å, respectively (which in turn are similar to the BP86/AE1 values in Table 2). The increased lability of the former water ligand is apparent from larger vibrational amplitudes along the trajectory (cf. the higher standard deviation of 0.14 Å, compared to 0.08 Å for V−O3) and from occasional notable displacements away from the metal (up to ca. 2.7 Å). However, the latter events were rare, and at no time during the total simulation of 5.5 ps was the water ligand liberated from the coordination sphere into the bulk.

Likewise, no water dissociation occurred for dicationic **1a** when this was placed in a periodic water box. Instead, a proton was transferred almost instantly from one water ligand to a nearby solvent molecule, affording a contact ion pair between an isomer of **2** and H_3O^+. When all six OH distances were fixed to their equilibrium values during the first 0.5 ps of equilibration and liberated thereafter, this proton transfer also occurred very rapidly, within ca. 100 fs after release of the constraint. Interestingly, the isomer of **2** that was formed did not correspond to **2a1**, the most stable six-coordinated form in the gas phase (Figure 2a and Table 2), but rather to **2a3**, interconverting with **2a4** via OH rotation about the V−O3 bond.

This result is in complete qualitative accord with those of the static computations discussed above, namely that **1** is a strong acid with a noticeable driving force for deprotonation yielding **2**. This result is also consistent with the experimental finding that **1** is best observed under highly acidic conditions. In order to model such an acidic solution, we have performed another CPMD simulation for **1a** in water, placing an additional proton in the box in order to mimic a solution that is about 1 M in acid. This simulation was started from a snapshot after the initial equilibration with fixed OH bonds, adding a proton to that water molecule that had, in the pure-water case, accepted the proton from the complex. Even though the resulting H_3O^+ ion was not stationary, but quickly relayed the proton to other, distant solvent molecules via the well-known shuttle mechanism,[47] **1a** underwent no permanent, irreversible deprotonations, at least not within the total simulation time of 6.5 ps. Reversible proton transfers were observed, however, but in all cases the transient contact ion pairs of **2** and H_3O^+ reverted to **1a** within ca. 0.1−0.4 ps. This fluxional character is illustrated in Figure 6, a plot of all six O−H distances in the three water ligands of **1a**. Transient proton transfers are easily identified by clearly visible spikes.

(45) Bühl, M.; Parrinello, M. *Chem. Eur. J.* **2001**, *7*, 4487−4494.
(46) There is evidence that gradient-corrected functionals such as BP86 tend to underestimate binding energies of water ligands with transition-metal−aquo complexes, cf.: Rotzinger, F. R. *J. Phys. Chem. B* **2005**, *109*, 1510−1527.
(47) (a) Tuckerman, M. E.; Laasonen, K.; Sprik, M.; Parrinello, M. *J. Chem. Phys.* **1995**, *103*, 150−161. (b) Marx, D.; Tuckerman, M. E.; Hutter, J.; Parrinello, M. *Nature* **1999**, *397*, 601−604.

Assigning an effective proton transfer to OH distances larger than 1.4 Å, the resulting isomers of **2** would be populated for roughly 20% of the time.

Even though no quantitative information regarding the equilibria between the various species can be drawn from the unconstrained CPMD simulations, the latter are consistent with the qualitative predominance of six-coordinate species **1** and **2** in water. These simulations further reproduce the finding that, unless stabilized by strongly acidic conditions, **1** is readily deprotonated to afford **2**. With this information at hand, we now proceeded to investigate potential modes of interconversion between selected isomers of **2**.

Mechanisms of Intramolecular Rearrangement Processes in $[VO(OH)U(H_2O)_2]^+$. It is likely that most of the minima for a given chelating ligand, e.g., **2a1**−**2c7** in Figure 2a, exist in various equilibria due to rapid intramolecular rearrangements. While the relative populations of all minima depend on their relative energies, their lifetime (and hence the possibility of individual detection, depending on the time scale of the analytical method) is governed by the activation energy of the respective interconversion. Since only very small barriers can be overcome in unconstrained MD simulations during a few picoseconds, we performed static optimizations in the gas phase to identify suitable reaction pathways.

We probed several possible rearrangement mechanisms in $[VO(OH)U(H_2O)_2]^+$ by locating the corresponding transition states, namely intramolecular and water-assisted 1,3-hydrogen transfer between water and hydroxyl ligands, intramolecular simultaneous transfer of two hydrogens involving two water and one hydroxyl ligands, intramolecular and water-assisted 1,3-hydrogen transfer between hydroxyl and oxo ligands, and water exchange with the solvent.

Among the most stable isomers of $[VO(OH)U(H_2O)_2]^+$, **2a1** (the global minimum) and **2a3** could interconvert by simple proton transfer between two adjacent water and hydroxy ligands. We have located the transition state $\mathbf{TS_{2a1-2a3}}$ for this process (Figure 7a), which contains a four-membered ring (4MR) with elongated O3−H and O4−H distances and a bridging O3−H−O4 angle of 136.8°. The only imaginary frequency of 942*i* cm^{-1} is associated with the movement of the bridging hydrogen between O3 and O4 atoms. In this case, we followed the intrinsic reaction coordinate (IRC)[48] and verified that $\mathbf{TS_{2a1-2a3}}$ indeed connects the desired minima, **2a1** and **2a3** (Figure 2a). At the BP86 level (including ZPE correction) the calculated energy barrier for the intramolecular 1,3-hydrogen migration between hydroxyl (O4) and water ligands (O3) in **2a** is 13.0 kcal/mol.

The energy demanding intramolecular 1,3-hydrogen migration may be circumvented by the active participation of a water molecule. It is well-established that the interconversion between isomeric ions in transition-metal chemistry can be catalyzed by their interaction with an appropriate neutral molecule, e.g., a water molecule.[49] The corresponding transition structure $\mathbf{TS_{2a2w-2a4w}}$ in such a water-assisted system (Figure 7b) rather resembles a $H_3O^+{\cdot}[VO(OH)_2U(H_2O)]$ complex, implying that the water molecule from the second solvation shell acts as a proton acceptor toward the water ligand (formerly involving, e.g., O3 in **2a1**). $\mathbf{TS_{2a2w-2a4w}}$ (Figure 7b) is characterized by a six-membered ring (6MR) which should be more favorable energetically than the 4MR in $\mathbf{TS_{2a1-2a3}}$ (Figure 7a). The minima connected by $\mathbf{TS_{2a2w-2a4w}}$ are microsolvated versions of **2a2** and **2a4** containing an additional water molecule in the second hydration sphere. We have chosen the microsolvated isomer **2a2w** as the reference point for this and all subsequent water-assisted rearrangements, since it is well within the small energetic span of the various isomers located so far (e.g., it is 1.21 kcal/mol more stable than the microsolvated analogue **2a1w**, and only 0.8 kcal/mol less stable than **2a4w**). It is a formidable task to locate the most stable isomer of a given complex microsolvated by one water molecule. However, little energetic discrimination is to be expected between these isomers, and we are confident that the reaction paths we have studied are representative for the particular intramolecular rearrangement process under scrutiny.

Relative to the hexacoordinated vanadium isomer **2a2w** the barrier via $\mathbf{TS_{2a2w-2a4w}}$ is only 1.8 kcal/mol, i.e., lower by ca. 10 kcal/mol than the intramolecular 1,3-hydrogen transfer (Table 6). There is thus a substantial catalytic effect of the additional water molecule, which can be attributed to a much reduced strain in the 6MR-transition structure compared to the 4MR one on the uncatalyzed reaction (illustrated by the calculated O3−V−O4 angles in $\mathbf{TS_{2a1-2a3}}$ and $\mathbf{TS_{2a2w-2a4w}}$, 69.6° and 90.1°, respectively, as compared to the value in **2a1**, 100.7°). The water molecule participates in the rearrangement by forming a bridge that facilitates the 1,3-hydrogen migration between O3 and O4 in $[VO(OH)U(H_2O)_2]^+$, and the energy barrier is markedly decreased (Table 6). In addition, we have localized three additional transition state structures (not shown) for the analogous rearrangement process, as indicated by their imaginary modes, but all these structures are higher in energy than $\mathbf{TS_{2a2w-2a4w}}$.

It is also possible that the addition of another water molecule in the second solvation sphere, as described earlier for the $VO(H_2O)^+$ isomer, could additionally reduce the corresponding energy barrier.[50] In that case an eight-membered ring would be formed enabling simultaneous transfer of two hydrogen atoms. The entropic penalty for such a highly ordered associate of three molecules, however, would be substantial, so that we have not explored this possibility further.

In both intra- and intermolecular processes, in which water ligands act as proton donors, it is assumed that the oxo ligand, due to its rather poor proton accepting property, is not involved in these rearrangement processes. This assumption

(48) (a) Gonzalez, C.; Schlegel, H. B. *J. Chem. Phys.* **1989**, *90*, 2154−2161. (b) Gonzalez, C.; Schlegel, H. B. *J. Phys. Chem.* **1990**, *94*, 5523−5527.

(49) East, A. L. L.; Smith, B. J.; Radom, L. *J. Am. Chem. Soc.* **1997**, *119*, 9014−9020.

(50) Sambrano, J. R.; Andrés, J.; Gracia, L.; Safont, V. S.; Beltrán, A. *Chem. Phys. Lett.* **2004**, *384*, 56−62.

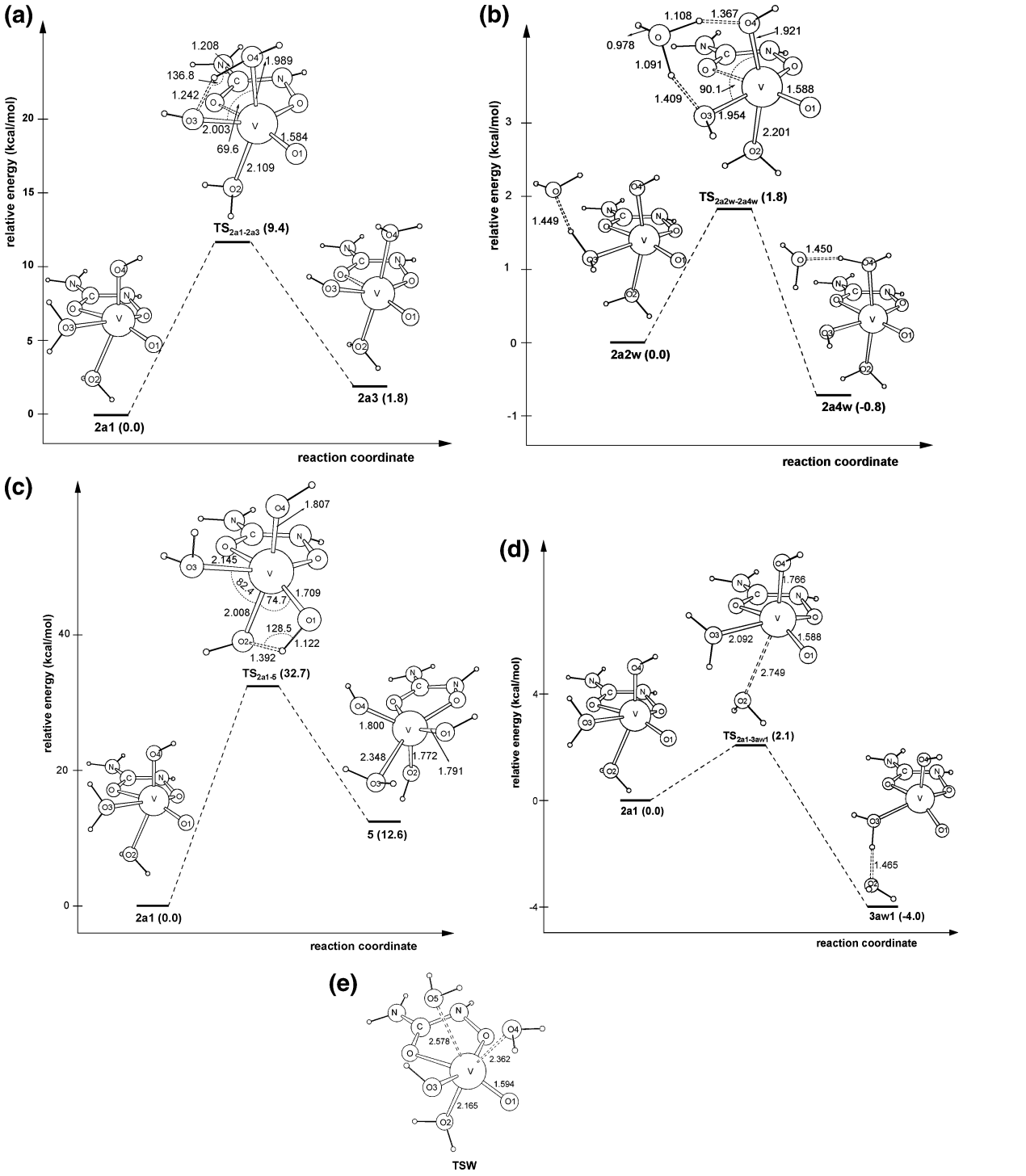

Figure 7. a. BP86 optimized transition state structure $\mathbf{TS_{2a1-2a3}}$ for intramolecular 1,3-hydrogen transfer betwen water and hydroxyl ligands in $[VO(OH)U(H_2O)_2]^+$. Distances are in angstroms, angles are in degrees. b. BP86 optimized transition state structure $\mathbf{TS_{2a2w-2a4w}}$ for the water assisted 1,3-hydrogen transfer between water and hydroxyl ligands in $[VO(OH)U(H_2O)_2]^+{*}H_2O$. Distances are in angstroms, angles are in degrees. c. BP86 optimized transition state structure $\mathbf{TS_{2a1\_5}}$ for intramolecular 1,3-hydrogen transfer from water to the oxo ligand in $[VO(OH)U(H_2O)_2]^+$. d. Transition state $\mathbf{TS_{2a1-3aw1}}$ for transfer of one water ligand in **2a1** to the second hydration sphere. e. BP86 optimized transition state structure TSW for water exchange process in $[VO(OH)U(H_2O)_2]^+$.

was tested by modeling the hydrogen atom transfer from one water ligand to the oxo ligand in **2a1**, affording isomer **5** $[V(OH)_3U(H_2O)]^+$ (Figure 7c). The computed energy barrier for this process **2a1** → **5** is 29.4 kcal/mol, which is indeed significantly higher than the barrier for the corresponding intramolecular hydrogen transfer between water and hydroxyl ligands **2a1** → **2a3**. The corresponding transition state structure $\mathbf{TS_{2a1-5}}$ has a highly strained 4MR characterized by elongated O1−H and O2−H distances (1.122 and 1.392 Å, respectively) and a bridging O1−H−O2 angle of 128.5° (Figure 7d). Isomer **5**, in which the oxo ligand is protonated (Figure 7c), was found to be 11.7 kcal/mol less stable than

Table 6. Electronic and Zero-Point Energies (in au), Together with Relative Energies (in kcal/mol) from Gas-Phase BP86/AE1 Calculations[c]

intramolecular rearrangements			water-assisted rearrangements[b]		
isomer	*E* (Hartree) ZPE	Δ*E* (kcal/mol)	isomer	*E* (Hartree) ZPE	Δ*E* (kcal/ mol)
2a1	−1547.87702 0.12313	0	**2a2w**	−1624.32687 0.14756	0
$\mathbf{TS_{2a1-2a3}}$	−1547.85864 0.11974 [977i cm^{-1}][a]	11.5 (9.4)	$\mathbf{TS_{2a2w-2a4w}}$	−1624.32395 0.14482 [370i cm^{-1}][a]	1.8 (0.1)
5	−1547.85694 0.12166	12.6 (11.7)	**2a4w**	−1624.32815 0.14332	-0.8 (-1.0)
$\mathbf{TS_{2a1\_5}}$	−1547.82497 0.11794 [1025i cm^{-1}][a]	32.7 (29.4)	**2a1w**	−1624.32495 0.14704	1.2 (0.9)
$\mathbf{TS_{2a1-2b1}}$	−1547.81083 0.11859 [2003*i* cm^{-1}][a]	41.5 (38.7)	$\mathbf{TS_{2a1w-2b1w}}$	−1624.31348 0.14541 [463*i* cm^{-1}][a]	8.4 (7.1)
$\mathbf{TS_{2a1-3aw1}}$	−1547.87375 0.12259 [110*i* cm^{-1}][a]	2.1 (1.7)	**TSW**	−1624.30069 0.14783 (93*i* cm^{-1})	16.4 (16.6)
3aw1	−1547.8833 0.12187	-4.0 (-4.8)			

[a] Imaginary frequency in transition state. [b] For plots of **2a1w** and **2b1w** see Figure S2 in the Supporting Information. [c] ZPE-corrected energies in parentheses.

2a1, suggesting that hydrogen migration from the water to the oxo ligand in **2a1** is both kinetically and thermodynamically unfavorable.

Hence, it is unlikely that rearrangement processes between isomers with equatorial and axial oxo groups would involve proton transfer from a coordinated water molecule to the oxo atom under formation of $[V(OH)_2U(H_2O)]^+$ intermediates such as **5**. Coordinated water ligands can transfer a proton only to OH groups, affording a scrambling of hydroxyl and water ligands positions.

Thus, for example, the isomers **2c7** and **2a1** with the oxo ligand in the *cis*- and the *trans*-positions (relative to the carbonyl of coordinated hydroxyurea), respectively, as well as the isomer **2b1** with the oxo ligand in the axial position are not expected to interconvert via hydrogen transfer from water to the oxo ligand.

However, the oxo ligand may be involved in rearrangements via hydrogen transfer from a hydroxyl ligand. These tautomerization processes, in which the oxo ligand is converted to a hydroxyl group and vice versa, could follow either an intramolecular or a water-asssisted mechanism, as described above for the hydrogen-transfer between water and hydroxyl ligands. The energy barrier for the most favorable intramolecular tautomerization (several analogous tautomerization processes were considered), in which the oxo ligand in the *cis*-position (relative to the carbonyl ligand) and the hydroxyl ligand in the axial position are interconverted, is calculated to be ca. 40 kcal/mol (relative to **2a1**). The corresponding transition state $\mathbf{TS_{2a1-2b1}}$ (Figure S1 in the Supporting Information), similar to $\mathbf{TS_{2a1-2a3}}$, is characterized by a strained 4MR. This energy demanding 1,3-hydrogen migration from the hydroxyl (O4−H) to the oxo ligand (O1) may be circumvented by the active participation of a water molecule, as described earlier.[51] Indeed, the energy barrier via $\mathbf{TS_{2a1w-2b1w}}$ (Figure S2) is significantly lowered to ca. 7 kcal/mol (relative to **2a1w** in Table 6) suggesting that tautomerization is also a fast rearrangement process. $\mathbf{TS_{2a1w-2b1w}}$ is characterized by elongated O4−H and O1−H distances (1.448 and 1.456 Å, respectively) and by shortened V−O1 and V−O4 bonds (1.661 and 1.665 Å, respectively). The OH bond of the water molecule involved in the hydrogen transfer process is also elongated (1.079 Å) as compared to the other OH bond (0.980 Å) not involved directly in this tautomerization.

The rearrangement of hexacoordinated isomer **2a1** to the corresponding pentacoordinated isomer proceeds via the transition state structure $\mathbf{TS_{2a1-3aw1}}$ (Figure 7d). This structure is one possible transition state for the interconversion process **2a1** → **3aw1** and describes the transfer of one water ligand from the first to the second solvation sphere (dissociation of water from the hexacoordinated isomer giving the microsolvated pentacoordinated isomer). This is essentially the same process that had occurred spontaneously in the CPMD simulation of gaseous **2a1** (see the preceding section and Figure 5). The structure $\mathbf{TS_{2a1-3aw1}}$ is characterized by a long O2−V distance of 2.749 Å. The only imaginary frequency is 110*i* cm^{-1} and is associated with the dissociation of water ligand from the hexacoordinated vanadium center. The calculated energy barrier for the process **2a1** → **3aw1** is 2.1 kcal/mol, similar to the value calculated for the analogous water elimination process in vanadate−dipeptide complexes.[32b]

Interestingly, this dissociation process **2a1** → **3aw1** is the most favorable intramolecular rearrangement (Table 6), unless the solvent water molecule is included as the catalyst in the water-assisted rearrangements.

Exchange rates between water molecules from the bulk solvent and those coordinated to transition-metal ions can vary substantially and have been used to classify the aqua complexes as labile or chest. It is possible that rearrangements of isomeric ions proceed via the water-exchange mechanism as reported previously.[52] For example, the results

(51) (a) Oliveira, J. A.; Almeida, W. B. De; Duarte, H. A. *Chem. Phys. Lett.* **2003**, *372*, 650−658. (b) Vallet, V.; Moll, H.; Wahlgren, U.; Szabó, Z.; Grenthe, I. *Inorg. Chem.* **2003**, *42*, 1982−1993.

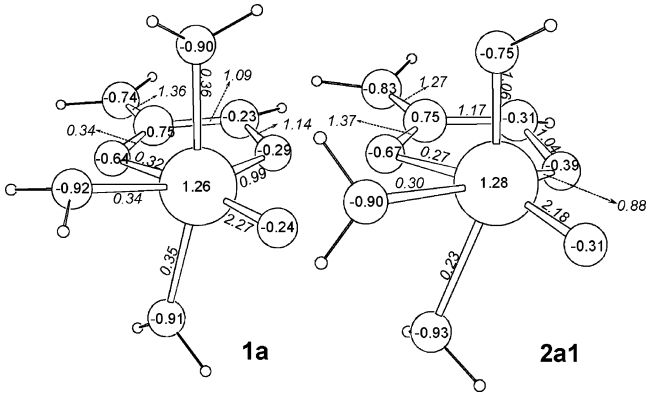

Figure 8. NPA charges (bold) and NBO Wiberg bond indices (given in *italics*) of complexes **1a** and **2a1**.

of DFT investigation on hexaaquavanadium(II) showed that the energy barriers for water exchange processes are higher in energy than 1,3-hydrogen migration.[53] We have located the transition state structure **TSW** for the water-exchange process in **2a3w** (Figure 7e); the corresponding energy barrier is calculated to be 16.6 kcal/mol (relative to **2a2w**), which is energetically the least favorable water-assisted type of rearrangement. In the transition state structure **TSW** two water molecules (O4 and O5), which exchange places, are loosely bound (with long $V-OH_2$ distances of 2.362 and 2.578, respectively) to the vanadium center. Because such degenerate water-exchange processes do not interconvert any isomers, however, they were not further explored. Likewise, rotational barriers of water and hydroxyl ligands about their V−O bonds, which also would isomerize certain isomers of **2**, were not computed, because very low barriers are expected for these processes.

To conclude this section, we have identified a variety of low-energy pathways for the interconverion of isomers of **2** via water-assisted proton transfers. Such transfers are indicated to be particularly facile between coordinated H_2O and OH groups and, as expected, to a lesser extent also between OH and oxo ligands. Even though rearrangement paths involving transient comproportionation of an oxo and a water ligand into two OH groups can be excluded, vanadium−hydroxamate complexes such as **2** are indicated to be quite fluxional systems.[54]

NBO Analysis of Isomers 1a and 2a1. Finally, we briefly discuss the electronic structures of the prototypical $[VO(OH)UH_2O]^+$ and $[VOU(H_2O)_2]^{2+}$ species **1a** and **2a1**, as assessed by calculated atomic charges and bond orders. The former are derived from natural population analysis (NPA), and the latter are evaluated as Wiberg bond indices (WBIs),[55] which are a probe for the covalent contributions to a particular bond. The results are summarized in Figure 8. Unsurprisingly, the calculated charges on the vanadium atoms are considerably lower than the formal charge +5. This is a result of significant charge donation from the oxo, hydroxy, and water ligands as well as from the *N*-hydroxyurea donor atoms. In both complexes **1a** and **2a1**, the charges of the terminal oxo ligand and those of the O atom in coordinated hydroxy or water ligands differ appreciably. The terminal oxo ligands are the least negative ones, which indicates the higher electron density delocalization from the terminal ligands toward the vanadium centers. The WBIs for the various V−O bonds decrease with an increasing negative charge on the donating O atom, indicative of the growing importance of ionic contributions to the bonding in the sequence $V-O < V-OH < V-OH_2$. WBIs are higher than 2 for bonds between the vanadium and terminal oxo ligands (2.27 and 2.18 for **1a** and **2a1**, respectively), around 1 for the V−OH and V−O(N) bonds in **2a1**, and between ca. 0.2−0.4 for the dative bonds involving water ligands and carbonyl O atoms.

Conclusion

We have used DFT calculations to study the monocationic and dicationic species, which result from complexation reactions between oxovanadium(V) and hydroxyurea and which coexist in fast proton exchange equilibrium.[18] A detailed conformational analysis was performed in order to identify the most stable isomer for a given compound, specifically pentacoordinated $[VO(OH)UH_2O]^+$ and $[VOU(H_2O)_2]^{2+}$ as well as the hexacoordinated $[VO(OH)U(H_2O)_2]^+$ and $[VOU(H_2O)_3]^{2+}$ complexes. As expected for weakly bonded species, the oxo, hydroxy, and water ligands display substantial conformational flexibility. In particular for the monocationic six-coordinate complexes, a large number of isomers was found in a relatively small energy range. The most stable species of both protonated and deprotonated forms of oxovanadium(V) complexes with hydroxyurea have the oxo atom in an equatorial position relative to the ring moiety and *trans* to the carbonyl oxygen. Bulk solvent effects, estimated from a polarizable continuum model, are relatively small and are not likely to change the relative stability of the different tautomers and conformers studied. Such simple continuum solvent models reach their limits when relative energies between complexes with different coordination number or, in particular, protonation states are concerned. These questions have been addressed with CPMD simulations in (explicit) aqueous solution. These simulations indicate that in water, six-coordination is favored over five-coordination, and that dicationic $[VOU(H_2O)_3]^{2+}$ is a strong acid, populated to a significant extent only in strongly acidic solution.

We have explored different pathways for interconversion between representative, low-lying hexacoordinate monocationic isomers. Several viable pathways were located, indicating that vanadate−hydroxyurea complexes can be quite fluxional. These pathways involve proton-transfer reactions between H_2O and OH or between O and OH ligands

(52) Rotzinger, F. P. *Chem. Rev.* **2005**, *105*, 2003−2037, and references therein.
(53) Benmelouka, M.; Messaoudi, S.; Furet, E.; Gautier, R.; Le, Fur, E.; Pivan, J.-V. *J. Phys. Chem. A* **2003**, *107*, 4122−4129.
(54) Single-point energy computations at the B3LYP/AE1 level afford somewhat higher barriers compared to the BP86 data (a typical effect of including Hartree-Fock exchange in the exchange-correlation functional). Even though this difference in computed barrier heights can approach ca. 8 kcal/mol in individual cases (see data in Table S5 of the Supporting Information), the qualitative conclusions (in particular concerning solvent assistance) are not affected.
(55) Wiberg, K. *Tetrahedron* **1968**, *24*, 1083−1096.

in the coordination sphere of vanadium. These processes are especially favorable when assisted by a water molecule from the second coordination sphere of the complex.

In summary, structure and speciation of vanadium(V) complexes with seemingly simple ligands is the result of a rich underlying chemistry, into which static and dynamic DFT computations can offer interesting and detailed insights.

Acknowledgment. The authors wish to thank Prof. Walter Thiel and the Max-Planck Society as well as the Croatian Ministry of Science, Education, and Sport for support. Computations were performed on a local compute cluster of Compaq XP1000, ES40, and Intel Xeon workstations and PCs at the MPI Mülheim and on an IBM regatta supercomputer at the Rechenzentrum Garching of the Max-Planck Society.

Supporting Information Available: Tables with optimized geometrical parameter and additional B3LYP energetic data, plots with stationary points of additional intramolecular rearrangement processes, and Cartesian coordinates of all complexes in xyz format. This material is available free of charge via the Internet at http://pubs.acs.org.

IC061699Y